

Effects of Baryon Mass Loss on Profiles of Large Galactic Dark Matter Haloes

Cinthia Ragone-Figueroa^{1*}, Gian Luigi Granato^{2†} & Mario G. Abadi^{1‡}

¹ *Instituto de Astronomía Teórica y Experimental, IATE, CONICET-Observatorio Astronómico, Universidad Nacional de Córdoba, Laprida 854, X5000BGR, Córdoba, Argentina*

² *Istituto Nazionale di Astrofisica INAF, Osservatorio Astronomico di Trieste, Via Tiepolo 11, I-34131 Trieste, Italy*

Accepted ... Received ...

ABSTRACT

We perform controlled numerical experiments to assess the effect of baryon mass loss on the inner structure of large galactic dark matter haloes. This mass expulsion is intended to mimic both the supernovae and AGN feedbacks, as well as the evolution of stellar populations. This study is meant in particular for precursors of massive Early Type Galaxies, wherein strong AGN feedback (often dubbed “QSO mode” in galaxy formation models) has been proposed to remove on a short timescale, of the order of a few dynamical times, a substantial fraction of their baryons. In a previous paper we evaluated the observational consequences (size increase) of this process on the galactic structure (Ragone-Figueroa & Granato 2011). Here we focus on the distribution of dark matter in the galactic region. It is shown that the inner region of the DM halo expands and its density profile flattens by a sizeable amount, with little dependence on the expulsion timescale. We also evaluate the effect of the commonly made approximation of treating the baryonic component as a potential that changes in intensity without any variation in shape. This approximation leads to some underestimates of the halo expansion and its slope flattening. We conclude that cuspy density profiles in ETGs could be difficult to reconcile with an effective AGN (or stellar) feedback during the evolution of these systems.

Key words: galaxies: formation - galaxies: evolution - galaxies: elliptical and lenticular, cD - galaxies: haloes - quasars: general - method: numerical

1 INTRODUCTION

A long standing puzzle of post recombination cosmology based on Cold Dark Matter, independently of the presence of cosmological constant or curvature in the adopted cosmological model, is the so called *core-cusp* problem (for a recent review see De Blok 2010). Since the 90’s, a long series of N-body (gravity only) simulations, dating back to Dubinsky & Carlberg (1991), has produced Dark Matter Haloes (DMH) whose inner density profile is reasonably well described by a power law $\rho \propto r^\alpha$ with $\alpha \sim -1$, i.e. a cusp. This is at odd with several observations, suggesting a flat density profiles of DM in the inner region of real galaxies, i.e. a core. The case for cored DM density profiles is rather strong in dwarf and disc dominated Low Surface Brightness (LSB) galaxies, wherein the dynamics of visible matter tracks safely the

largely dominating gravitational field of DM. Also the dynamics of normal spiral galaxies is best interpreted by means of cored DM mass models (e.g. Salucci & Frigerio-Martins 2009 and references therein), while the presence of a core in DMH of large elliptical galaxies is difficult to assess and controversial (e.g. Memola, Salucci & Babić 2011; Sonnenfeld et al. 2011; Tortora et al. 2011), since their central region is even more gravitationally dominated by the baryon component, and because of the less straight-forward to interpret orbital structure.

A widespread idea is that the solution of the core-cusp problem should be searched for in the physics of baryonic matter, that can affect to some extent the distribution of DM in the inner region of haloes, and is not included in the aforementioned computations.

However, the first baryonic process expected to occur worsen the problem. It consists in some further contraction of the central region of the DMH, induced by the much stronger concentration-collapse of dissipative baryonic matter (e.g. Blumenthal et al. 1986; Gnedin et al. 2004;

* Email: cin@oac.uncor.edu

† Email: granato@oats.inaf.it

‡ Email: mario@oac.uncor.edu

Abadi et al. 2010, Gnedin et al. 2011). The exact importance of this process is somewhat debated. Different numerical works found different results, and significantly less contraction than that predicted by the simple analytic estimate by Blumenthal et al. (1986). In any case, this mechanism produces some further steepening of the inner profile, with respect to the prediction of gravity only cosmological simulations.

Nevertheless, several subsequent (and more complex) baryon processes occur after this primary condensation, and can act in the opposite direction. Indeed, they have been often evaluated specifically to seek solutions to the core-cusp problem (e.g. Navarro, Eke & Frenk 1996; Gnedin & Zhao 2002; Read & Gilmore 2005; Tonini, Lapi & Salucci 2006; Mashchenko, Couchman & Wadsley 2006; Mashchenko, Wadsley & Couchman 2008; Pasetto et al. 2010; Governato et al. 2010; De Souza et al. 2011; Ogiya & Mori 2011; Inoue & Saitoh 2011; Martizzi et al. 2011; Pontzen & Governato 2012; Macciò et al. 2012). Several of these papers have addressed the effect of baryon ejection, due to SNaE feedback, on the central DM density profile of less massive systems, i.e. mainly dwarfs or at most disk dominated galaxies. The results on its importance have been sometimes contradictory (for a discussion of possible causes, see Read & Gilmore 2005).

Much less attention has been paid so far to these effects in larger systems, such as Early Type Galaxies (ETGs). The main reason is obviously that their DM content is less constrained by the data, as noted above (for a review see Buote & Humphrey 2012). Moreover, mechanisms related to SNaE feedback are expected to be less effective in the deeper potential wells of large ETGs. As for the first point, it is worth noticing that recent observational evidence points either to a DM distribution shallower (Memola, Salucci & Babić 2011) or cuspier (Sonnenfeld et al. 2011; Tortora et al. 2012) than that predicted by Λ CDM gravity only simulations. New techniques could soon provide constraints on the DM distribution in ellipticals (e.g. Pooley et al. 2011). As for the second point, in the past few years it has become common to consider in galaxy formation theory the feedback of AGN activity, which is likely to be much more effective in massive systems than that due to SNaE (e.g. Silk & Rees 1998; Fabian 1999; Granato et al. 2001, 2004; Benson et al. 2003; Cattaneo et al. 2006; Monaco et al. 2007; Sijacki et al. 2007; Somerville et al. 2008; Johansson et al. 2009; Ciotti, Ostriker & Proga 2009). AGN feedback is widely considered the most promising mechanism for relaxing those tensions between galaxy formation models and observation, broadly related to the so called *overcooling problem*. This is the tendency of models to produce too massive and too blue (i.e. star forming) galaxies at low redshift, and to lock up in galaxies an excessive fraction of available baryons. On the contrary, many observations indicate that on average the more massive a galaxy, the earlier it stops its star formation activity, a phenomenon referred to as *downsizing* (e.g. Brammer et al. 2011; for a critical discussion of the various manifestations of downsizing see Fontanot et al. 2009). Despite the likely prominent role of AGN feedback in galaxy formation, so far its effect on the DM distribution has not been evaluated in detail (but see Peirani, Kay & Silk 2008 and Duffy et al. 2010).

One kind of AGN feedback (that sometimes called

”QSO mode”) is expected to eject on a small timescale (of the order of a few 10 Myr at most) the cold gas not yet converted into stars in star forming ETGs. In a recent work (Ragone-Figueroa & Granato 2011; henceforth Paper I) we have evaluated with aimed numerical simulations the importance of this process, concentrating our analysis on the baryon component of ETGs, in order to assess its possible contribution to the observed size evolution of ETGs (see e.g. Newmann et al. 2011 and references therein). In this paper we investigate instead in detail the effects on the profile of the DM halo.

Since we are mainly interested in ETGs rather than less massive systems such as dwarfs, we will extend the studies already published to regions of the parameter space not covered previously. Indeed, this is the first work where the initial conditions have been thought to get a configuration, after the loss of a substantial fraction of baryons previously condensed in the central region of the DM halo (i.e. the galactic region), consistent with our basic knowledge of the properties of local large ETGs (baryon to DM mass ratio, scalelengths, size as a function of stellar mass). By converse, in most studies the baryons totally disappear, or the remaining fraction is $\leq 5\%$, consistently with the very low baryon content of dwarf galaxies. This is not the case for ETGs, where the leftover baryons still dominate the potential wells in the central region of the DM halo. Also, in order to assess the maximal effect of baryon loss, in most studies the initial mass ratio of condensed baryon to DM has been set close to the cosmic baryon fraction. However this appears too extreme, at least for ETGs. According to the cooling prescriptions adopted by semi analytic models and simulations of galaxy formation, no more than a few tens percent of the cosmic baryons had time to cool and condense in a large galactic DM halo, during the few Gyrs over which ETGs formed at $z \gtrsim 1.5$ (e.g. Benson et al. 2001; Helly et al. 2003; Granato et al. 2004; Cattaneo et al. 2007; Viola et al. 2008). We point out explicitly that the results of previous numerical experiments, when featuring substantial differences in the initial and/or final mass ratios of baryon to DM, or in the assumed density profiles of the two components (often disks for the baryons), cannot be simply re-scaled to predict quantitatively our findings.

Moreover, a technical difference with respect to most previous similar works is that often the baryon component has been treated as a fixed shape (rigid) potential. Here in general we do not adopt this approximation (since in Paper I we wanted actually to study the expansion of leftover baryons), but we evaluate its effect.

The organization of the paper is straightforward: in Section 2 we describe the initial conditions and method for our simulations, whose result are presented in Section 3. The implications for our understanding of ETGs formation are discussed in Section 4.

2 NUMERICAL METHOD AND SETUP

The setup of the simulations used in this paper is similar to that described in Paper I, to which we refer for a few more details. The main difference is that here we run also simulations in which the initial conditions take into account the possible halo contraction due to baryon condensation.

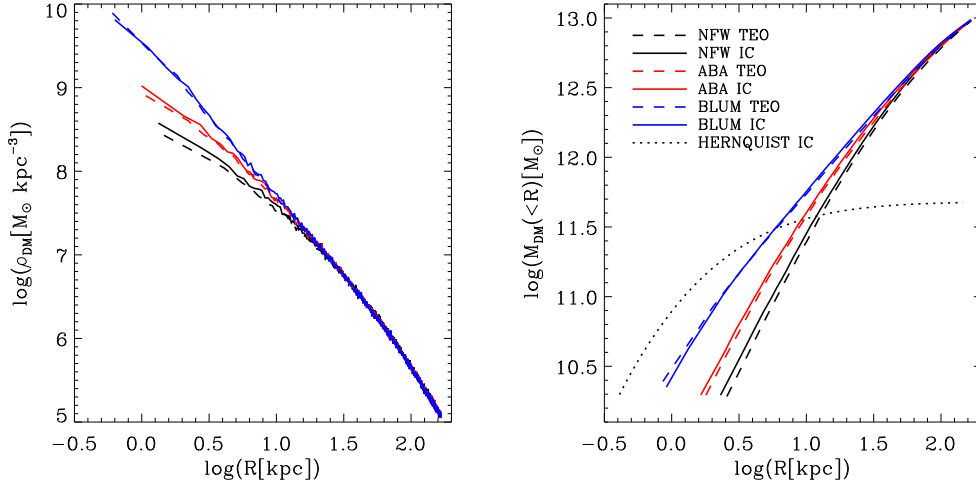


Figure 1. The curve marked NFW TEO represents the typical density run of DM haloes produced by gravity only simulations (Navarro, Frenk & White 1997), whilst ABA TEO and BLUM TEO are intended to keep into account the contraction resulting from galaxy formation, as described in Section 2. After setting these theoretical initial conditions (dashed lines in both panels) we let each system to evolve, for 0.4 Gyr, to an equilibrium configuration. These are considered the initial conditions (IC) for the numerical experiments before forcing baryon mass loss. The density and mass profiles are shown in the left and right panel, respectively. In addition we show in the right panel the mass Hernquist profile corresponding to the baryonic component.

Moreover, we evaluated the effect of the approximation of treating the baryons as a fixed shape potential.

The purpose of the simulations is to investigate the evolution of collision-less particles (stars and DM) under a change of gravitational potential due to a loss of baryonic mass of the system. In general, the escaping mass can represent either the gas which has not been converted into stars during the star forming phase of the spheroid (ejected by feedback driven galactic winds), or the mass lost from stars in form of stellar winds and SNa explosions (which is likely to escape the ETGs potential wells). In any case, we assume as given, and due to causes not included in our physical treatment (such as SNa and AGN feedbacks, or stellar evolution), the temporal dependence of this mass loss (Eq. 10), which we put by hand, and we simulate the ensuing dynamical evolution of collision-less mass distributions. Therefore we don't have to treat the gas dynamics.

We used the public version of the code *GADGET-2* (Springel et al. 2005) to perform simulations with 10^6 and 5×10^6 particles, in the gravity only mode. None of the presented results shows any noticeable difference in the two cases, which assures us that the mass resolution is sufficient for the purposes of the present study. Half of the particles are used to sample the baryonic and dark matter components respectively, with a softening of 0.007 and 0.35 kpc respectively. We checked that our results are not affected by significant variations in these choices.

The density distribution of DM particles is initially (i.e. even before computing the effects of baryonic contraction; see below) assumed to follow the standard NFW (Navarro, Frenk & White 1997) shape

$$\rho_{\text{DM}}(r) = \frac{M_{\text{vir,DM}}}{4\pi R_{\text{vir}}^3} \frac{c^2 g(c)}{\hat{r} (1 + c\hat{r})^2}, \quad (1)$$

where $M_{\text{vir,DM}}$ is the halo virial mass in DM (the DM mass

inside R_{vir}), $\hat{r} = r/R_{\text{vir}}$, c is the concentration parameter and $g(c) \equiv [\ln(1+c) - c/(1+c)]^{-1}$.

The virial radius R_{vir} is by definition the radius within which the mean density is $\Delta_{\text{vir}}(z_{\text{vir}})$ times the mean matter density of the universe $\rho_u(z_{\text{vir}})$ at virialization redshift z_{vir} :

$$R_{\text{vir}} = \left[\frac{3}{4\pi} \frac{M_{\text{vir}}}{\Delta_{\text{vir}}(z_{\text{vir}})\rho_u(z_{\text{vir}})} \right]^{1/3}, \quad (2)$$

The overdensity $\Delta_{\text{vir}}(z)$, for a flat cosmology, can be approximated by

$$\Delta_{\text{vir}}(z) \simeq \frac{(18\pi^2 + 82x - 39x^2)}{\Omega(z)}, \quad (3)$$

where $x = \Omega(z) - 1$ and $\Omega(z)$ is the ratio of the mean matter density to the critical density at redshift z (Bryan & Norman 1998). The corresponding mass distribution is written

$$M_{\text{DM}}(<r) = M_{\text{vir,DM}} g(c) \left[\ln(1 + c\hat{r}) - \frac{c\hat{r}}{(1 + c\hat{r})} \right]. \quad (4)$$

For the collisionless baryonic particles (representing the potential of both stars as well as gas before expulsion), we assume that, as a result of the assembly of the central galaxy, they settle on an Hernquist (1990) profile, which provides a reasonable description of stellar density in spheroids:

$$\rho_{\text{B}}(r) = \frac{M_{\text{B}}}{2\pi} \frac{a}{r} \frac{1}{(r+a)^3}; \quad (5)$$

where M_{B} is the total baryonic mass. The corresponding mass distribution is

$$M_{\text{B}}(<r) = M_{\text{B}} \left(\frac{r}{r+a} \right)^2; \quad (6)$$

so that the half-mass radius is related to the scale radius a by $R_{1/2} = (1 + \sqrt{2})a$ and, assuming a mass to light ratio independent of r , the effective radius is $R_e \simeq 1.81a$.

As discussed in the introduction, the process of baryon

condensation in the centre of the DMHs is expected to contract to some extent the DM distribution. Since, at variance with Paper I, the target of this study is precisely to evaluate the effect of baryon expulsion on DMH density profiles, we performed also runs including an estimate of the contraction in the initial conditions, by adopting the Abadi et al. (2010) prescriptions. They found that a simple formula captures the average behavior of their simulations:

$$r_f/r_i = 1 + \alpha [(M_i/M_f)^n - 1] \quad (7)$$

where n and α are parameters (see below). This equation relates the initial (i.e. before baryon condensation) and final radii of the spheres containing the same amount of DM, to the total masses M_f and M_i within the same spheres. Since

$$\frac{M_f}{M_i} = \frac{M_{f,DM}(< r_f) + M_{f,bar}(< r_f)}{M_{i,DM}(< r_i) + M_{i,bar}(< r_i)} \quad (8)$$

where $M_{f,DM}(< r_f) = M_{i,DM}(< r_i)$, by definition of r_i and r_f . Once it is assumed an initial density distribution for DM and baryons and a final density distribution for baryons, Eq. 7 is an implicit equation for r_f given an r_i , that can be solved numerically to obtain the final mass distribution of DM, $M_{f,DM}(< r)$. As stated by Abadi et al. (2010), their results are well described setting $n = 2$ and $\alpha = 0.3$. Moreover the contraction predicted by Blumenthal et al. (1986), as well as that found in simulations by Gnedin et al. (2004), are well described setting $n = 1$, and $\alpha = 1$ or $\alpha = 0.73$ respectively. When exploiting Eq. 7, we describe the initial mass distribution of DM and the final mass distribution of baryons with Eq. 4 and Eq. 6. Also, we assume that before contraction baryons follow the same density distribution of DM (Eq. 1), rescaled by the cosmic baryon fraction we assume $f_b = \Omega_{bar}/\Omega_m = 0.17$ (consistent with CMB WMAP-7 constraints, Komatsu et al. 2009).

In the following, unless otherwise specified, by *dynamical time* t_{dyn} we mean the initial (i.e. before any mass loss and expansion) dynamical time, computed at baryon $R_{1/2}$.

$$t_{dyn} = \left[\frac{R_{1/2}^3}{2G (M_B/2 + M_{DM}(< R_{1/2}))} \right]^{1/2} \quad (9)$$

Even though in this paper our focus is on the evolution of the DM component of the system, we maintain the same definition of dynamical time as in Paper I, since the effects under study are confined to the inner region of the DM distribution.

Given the density profiles, we obtain the 1D velocity dispersion by integrating the Jeans equation under the assumption of isotropic conditions. To generate initial conditions, we randomly populate the system with baryonic and DM particles, according to the density distributions Eq. 5 and Eq. 1. The particles velocities are randomly generated assuming local Maxwellian distribution, with 1D velocity dispersion obtained by the solution of Jeans equation. Then, by numerically evolving the system for several dynamical times, we obtain a (quasi)-static statistical equilibrium. This latter step does not produce significant variations in the density profiles (see discussion of Fig. 1 in Section 3 for more details).

Starting from this initial setup, we introduce a mass loss, by removing exponentially during an ejection time interval Δt a fraction $1 - \epsilon$ of the baryonic mass :

$$M_B(t) = M_{B(t=0)} \exp\left(\frac{\ln \epsilon}{\Delta t} t\right) \quad (10)$$

The mass loss is practically attained by decreasing correspondingly in time the mass of the baryonic particles sampling the density field. After the end of the mass loss period Δt , we let the system to evolve till it reaches a new equilibrium configuration.

We wanted also to study the effect of a common approximation done when evaluating the evolution of the DM distribution under a baryon mass loss, namely to treat the baryonic component as a potential that changes in intensity without any variation in shape (a rigid potential; e.g. Navarro et al. 1996; Ogiya & Mori 2011). For this purpose, we run also simulations in which the positions of baryonic particles were not updated in time.

The reference value for the initial (i.e. before any mass loss) ratio of virial mass (total mass within the virial radius) to baryonic mass is $M_{vir}/M_{B(t=0)} = 20$. This value is in keeping with the fraction 20%-40% of cosmic baryons that can cool and condense in the central region of a large galactic DM halo at $z \gtrsim 1.5$, according to the prescriptions adopted by semi analytic models and simulations of galaxy formation (e.g. Benson et al. 2001; Helly et al. 2003; Granato et al. 2004; Cattaneo et al. 2007; Viola et al. 2008). Moreover, assuming that after the initial condensation the halo looses, due to feedback induced galactic winds, a fraction between 20% to 80% of this "galactic" baryonic mass, it is left with a baryon to DM content broadly consistent with estimates in the local universe for large galactic haloes (Monster et al. 2010).

We set $M_{vir} = 10^{13} M_\odot$ in all simulations. Nevertheless, our results apply to different values of M_{vir} , provided that the ratios of scale radii and masses in the two components (DM and baryons) are not changed, and that the time is measured in units of dynamical time $t_{dyn} \propto \rho^{-1/2}$.

We adopt a concentration parameter $c = 4$, a typical value at galactic halo formation (see Zhao et al. 2003; Klypin, Trujillo-Gomez, & Primack 2010), and $R_{vir} \simeq 170$ kpc (from Eq. 2 and Eq. 3, with $M_{vir} = 10^{13} M_\odot$ and $z_{vir} = 3$).

Finally, we set $a = 1.5$ kpc ($R_e \simeq 2.7$ kpc). We refer the reader to Section 3 of Paper I for motivations for this values. The initial (i.e. before mass loss and expansion, Eq. 9) dynamical time as defined above is $t_{dyn} \approx 5$ Myr.

In summary, the parameters affecting the results of our simulations are the ratio of mass between the total and baryonic components $M_{vir}/M_{B(t=0)}$; the corresponding ratio of scale-lengths R_{vir}/a ; the fraction of baryonic mass lost $(1 - \epsilon)$, and the time Δt over which the loss occurs. We performed simulations covering broad ranges of the latter two quantities, while in most runs we kept the former two at the fiducial values reported above. We checked however that none of our qualitative conclusion is affected by factor ~ 2 variations of them (Paper I and some more discussion in Section 3).

3 RESULTS

Fig. 1 shows the initial equilibrium density and mass profiles for the DM component, i.e. those adopted before forcing any

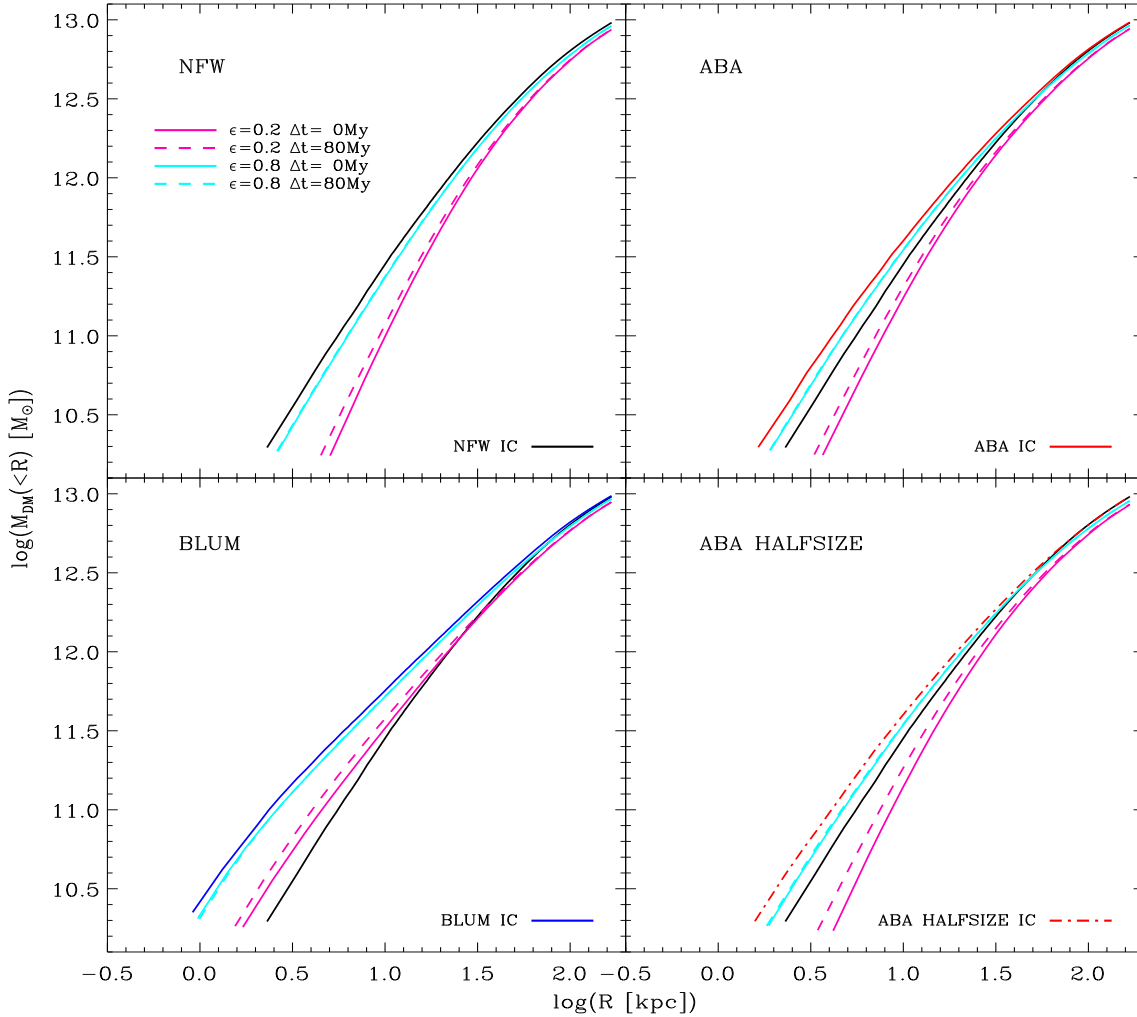


Figure 2. Comparison between the initial and final mass profiles. The latter is the new equilibrium configuration reached ~ 0.2 Gyr after the baryonic mass loss (see Fig. 4). Each panel refers to simulations performed adopting a different initial density profile, as indicated by the inner label, which is plotted with the same color as in previous figure. ABA HALFSIZE IC (bottom right panel) is obtained as ABA IC, but halving the Hernquist scale radius of the baryonic component. The final profiles for $\epsilon = 0.2$ and $\epsilon = 0.8$ are in magenta and cyan respectively; solid lines are for $\Delta t = 0$ Myr (instantaneous baryon expulsion) and dashed lines for $\Delta t = 80$ Myr (barely distinguishable for the lower mass loss $\epsilon = 0.8$). In all panels we plot for reference also the standard NFW profile (black solid line).

loss of baryonic mass (solid lines). The right panel also displays the adopted standard Hernquist mass profile for the baryons. Here and in the following, the lower limit of the density and mass profile plots equals the adopted gravitational softening for the DM component, the density and the accumulated mass are evaluated using radial bins containing $\simeq 500$ DM particles. These initial profiles are obtained letting to evolve for several tens of dynamical times the composite system, where for the DM component we adopted the pure NFW mass profile (black dashed line), or the profiles implicitly given by Eq. 7, with values of the n and α parameters adequate to reproduce the contraction found by Abadi et al. (2010) in simulations (red dashed line) or that analytically predicted by Blumenthal et al. (1986) (blue dashed line), as detailed in Section 2. We refer to these three cases as NFW, ABA and BLUM respectively. The first and the last should be regarded as extreme cases where the effect

of contraction is negligible and maximal, respectively, while the intermediate case, ABA, is likely to be more realistic. The numerical evolution does not affect much the initial configuration of DM. For instance, the local power law index of the density distribution increases in the inner ~ 10 kpc by less than 0.1, making it slightly steeper. The effect decreases with increasing contraction of the DM profiles, i.e. from NFW to BLUM. Kazantzidis, Magorrian & Moore (2004) suggested that the local Maxwellian assumption employed here (and in many other works) to set up the initial conditions, can lead to spurious results in the study of long term evolution of DM haloes. In particular they found that the central cusp is quickly significantly reduced. In our case we find a much less important, and opposite, trend. We attribute this to the presence of the dominating baryonic component in the center of the halo, not included in the study by Kazantzidis et al. Indeed, on one hand we run a pure

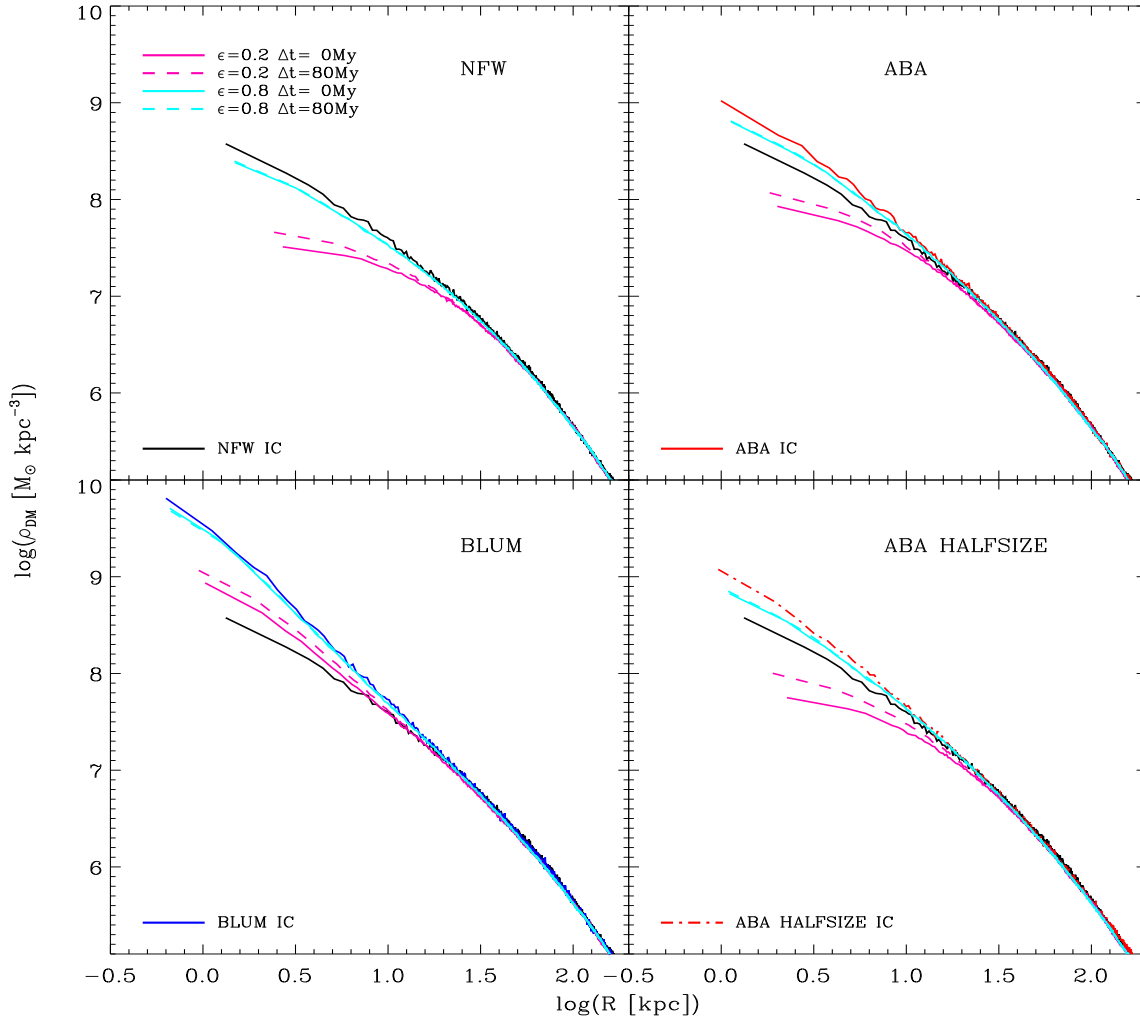


Figure 3. The same as the previous figure but comparing the initial and final density profiles. The different panels correspond to different ICs as labeled in the plot.

DM test case, which confirmed their result on the reduction of the central cusp. On the other hand, we note that also Read & Gilmore (2005), who considered composite baryon plus DM systems as we did, found excellent agreement between initial conditions generated with the Maxwellian approximation and with the alternative procedure proposed by Kazantzidis et al. (2004).

In addition to the three cases NFW, ABA and BLUM, and in order to study the dependence of our results on the parameters of the initial baryonic configuration, we considered ICs in which we halved the scale radius of the baryonic component (henceforth ABA HALFSIZE) or we doubled its mass. We then correspondingly contract the DM halo as we did for ABA. The direction of these variations has been elected in order to increase the effect of mass loss with respect to the standard case. These two initial conditions are not shown in Fig. 1, since they are almost indistinguishable from ABA IC.

Fig. 2 and Fig.3 display the effect of baryon mass loss on the initial mass distributions described above. The four panels in each figure correspond to the ICs dubbed NFW,

ABA, BLUM and ABA HALFSIZE. The new equilibrium configurations, shown in the figures, are reached typically a few tens of dynamical times (Eq. 9) after the end of the mass loss period (Δt), as can be appreciated in Fig. 4. Whenever the fraction of baryon lost is important (say $\gtrsim 50\%$), the final DM profile is significantly flatter in the center than the initial one. If this is the case, the ensuing expansion more than counteracts the opposite contraction caused by baryon condensation, at least that found in recent numerical simulations (Abadi et al. 2010), see right panels. The effect is somewhat weaker when the DM profile is initially more concentrated, as expected since in this case the contribution of DM to the gravitational field in the center becomes more important. For the same reason, the flattening effect in ABA HALFSIZE is slightly enhanced with respect to ABA. Indeed, in the former ICs, the contribution to the initial equilibrium of the baryons that we let to escape during mass loss was higher. To a lesser extent, the same happens doubling the initial baryon mass, but the difference is barely visible, so that we don't plot this case.

The dependence on the timescale of the mass loss is

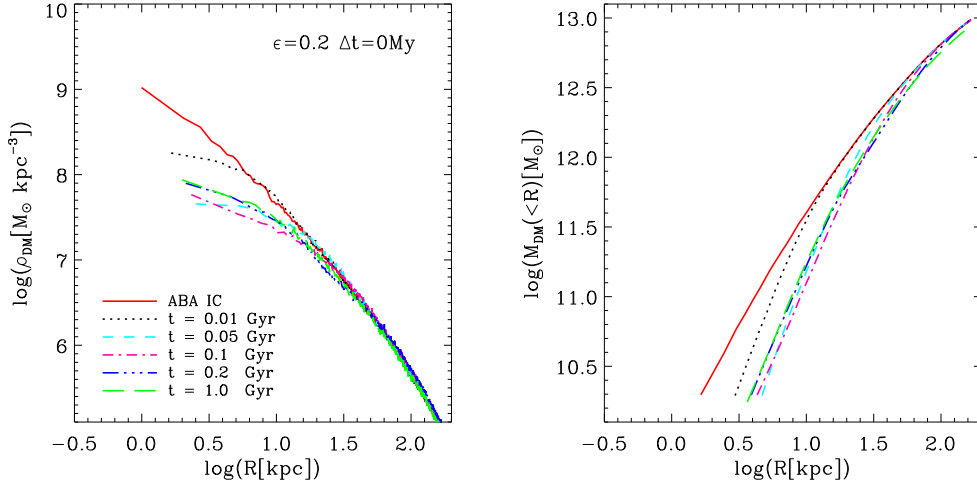


Figure 4. Time evolution, after the baryon mass loss, of the density (left panel) and mass (right panel) DM profiles for one of our simulations, namely the case ABA with instantaneous mass loss $\Delta t = 0$ Gyr and $\epsilon = 0.2$. The new equilibrium is reached within ~ 0.2 Gyr, i.e. within 40 dynamical times of the central region, Eq. 9. This holds true for all the other cases.

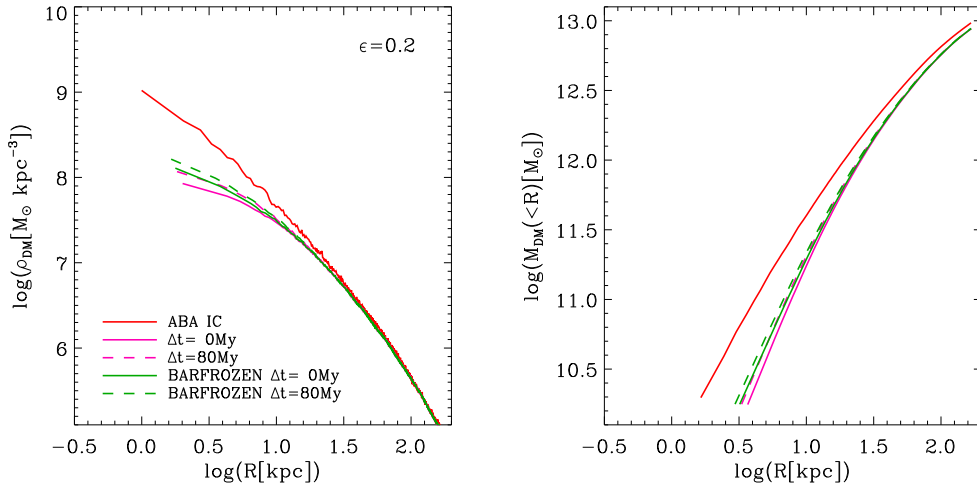


Figure 5. Comparison between the new equilibrium DM density (left panel) and mass (right panel) profiles after baryon mass loss, for $\epsilon = 0.2$, obtained letting the baryon particles to adjust their position according to the change of potential (magenta lines), or keeping their position fixed (green lines). The former is the treatment adopted in this work, while the latter corresponds to the common approximation of treating the baryons as a rigid potential.

weak. This finding is at variance with respect to the result by Ogiya & Mori (2011), who found that if the loss is slow enough, the DM profiles are much less affected, up to the point that after a while it returns very close to the initial conditions. We have checked that this result is not due to the approximation used by Ogiya & Mori of treating the baryons as a fixed form potential (see below). This difference could arise in part, but not entirely, from the more compact baryon distribution adopted by these authors. Actually, we find a somewhat more evident dependence on timescale when the baryon component is initially more concentrated (ABA HALFSIZE; lower right panels). It is also interesting to note that the expansion of the baryonic mass distribution

is much more affected than that of the DM by the timescale of expulsion (see Paper I for details).

In Fig. 4 we show the time evolution of the density (left panel) and the mass (right panel) profiles of a representative model, after the baryon mass loss. The chosen run corresponds to the case ABA with instantaneous mass loss $\Delta t = 0$ Gyr and $\epsilon = 0.2$. The figure shows that the profile at remains stable after ~ 0.2 Gyr. The new equilibrium is reached within 40 dynamical times of the central region (Eq. 9). This holds true for all the other simulated cases.

A commonly made approximation in evaluating the effect of baryon expulsion (or condensation) on the DM halo is to treat the baryonic component as a potential that changes in intensity without any variation in shape. Fig. 5 illustrates

that this approximation leads to some underestimate of the slope flattening and of its (weak) dependence on the expulsion timescale. This is due to the fact that the mass loss actually causes a significant broadening of the baryon concentration in the centre, which changes the shape of the potential and is more important for shorter timescales (Paper I). Therefore, in the full computation, the DM distribution is flattened not only by the decrease of gravitational force of baryons, but also by the (timescale dependent) outside dragging, due to the expansion of the leftover baryonic matter.

4 DISCUSSION AND CONCLUSIONS

A well known general prediction of cosmological, gravity only, simulations is that DM haloes should have cuspy density profiles, essentially independently of the mass scale¹. Observations at small to medium galactic scales (dwarf galaxies, disc dominated LSB galaxies, as well as normal spirals) have demonstrated that this is not the case. At cluster scales, where DM is gravitationally subdominant in the central region, the situation is instead far from clear, with several claims for cored (e.g. Richthel et al. 2011) as well as for cuspy (e.g. Zitrin et al. 2011) density profiles. The former mismatch is widely ascribed to the back-reaction of baryons, whose evolution to form galaxies is driven by various non-gravitational processes, on DM particles. The intermediate regime of large ETGs, the subject of our work, has received so far much less attention, both from the observational as well as the theoretical point of view. As for the former, again there are interpretations favoring a cored (e.g. Memola et al. 2011) as well as a cuspy (Tortora et al. 2010, Sonnenfeld et al. 2011) density profile. Firm conclusions are however severely plagued by the degeneracy between the Initial Mass Function (IMF) and the DM density profiles (Treu et al. 2010).

In the present paper, we have elucidated that an important gas removal during the early evolution of ETGs, should leave as a byproduct sizeable signatures also on the inner profile of their DM haloes. A similar ejection is required by most galaxy formation models aiming to explain the basic properties of these systems, such as their chemical properties, low baryon content or luminosity function (e.g. Benson et al. 2003; Granato et al. 2004; Pipino, Silk & Matteucci 2009; Duffy et al. 2010), and it is commonly, but not always, ascribed to *QSO mode* AGN feedback. The DM density profile ends up to be significantly less concentrated than NFW, unless the prior (opposite) contraction generated by baryon collapse and condensation has been very efficient, and probably unrealistic, i.e. closer to that estimated on the basis of approximate analytical treatments (e.g. Blumenthal et al. 1986), than to that found in most cosmological simulations (e.g. Abadi et al. 2010; Gnedin et al. 2011).

Moreover, it has been pointed out that stellar feedback can weaken the DM cusp in dwarf and spiral galaxies not only by means of gas removal from the galaxy potential well, but also as a consequence of oscillations of the potential generated by bulk motions of gas within the galaxy

¹ note that this feature has been found recently also in self-similar analytic models for the halo collapse (e.g., Lapi & Cavaliere 2011).

(Mashchenko et al. 2006, 2008; Potzen & Governato 2012; Macciò et al. 2012). As for the AGN feedback, similar fluctuations could be induced, for instance, by non isotropic gas removal. Although, for simplicity and lack of theoretical understanding, models of galaxy formation treat AGN feedback by means of isotropic sub-grid prescriptions, the case for preferential directions for the effect of AGN activity on its environment is actually strong. Indeed, all our knowledge of the AGN phenomenon points to a non isotropic structure, including accretion discs, jets, ionizations cones and dust tori. More specifically, recent observational evidence directly indicates non isotropic quasar driven gas removal (e.g. Cano-Diaz et al. 2011). To explore properly this effect would require more complex numerical experiments, possibly including a treatment of gas dynamics. The effort seems somewhat premature at present, given the lack of understanding of how AGN gas removal works, and we leave it for future investigations². In any case, it is worth noticing that this possible additional process could even enhance the flattening effect of AGN feedback on the DM distribution estimated here.

Martizzi et al. (2011) suggested that several mechanisms contribute to the formation of the ~ 10 kpc core in the Brightest Cluster Galaxy of a simulated Virgo-like galaxy cluster ($M_{vir} \simeq 10^{14} M_{\odot}$), found when (and only when) sub-grid models for the growth of SMBHs and the ensuing feedback are included in their hydro-simulation. Our idealized numerical experiments elucidates and quantifies the important contribution of one of these mechanisms, namely the ejection of baryonic matter (representing gas).

In conclusion, cuspy density profiles in ETGs, tentatively inferred from some recent observation, could be difficult to reconcile with an effective AGN (or stellar) feedback, in particular that believed to cause massive galactic winds during the early evolution of these systems, making them *red and dead*.

ACKNOWLEDGMENTS

C.R-F. and G.L.G. acknowledge warm hospitality by INAF-Trieste and IATE-Córdoba, respectively, during the development of the present work. We thank A. Lapi, P. Salucci, J. Navarro and A. Meza for several useful discussions on the topic of this work. This work has been partially supported by the Consejo de Investigaciones Científicas y Técnicas de la República Argentina (CONICET), by the Secretaría de Ciencia y Técnica de la Universidad Nacional de Córdoba (SeCyT) and by the European Commissions Framework Programme 7, through the International Research Staff Exchange Scheme LACEGAL.

REFERENCES

Abadi M. G., Navarro J. F., Fardal M., Babul A., Steinmetz M., 2010, MNRAS, 407, 435

² Peirani et al. (2008) performed idealized numerical experiments partly in this spirit, in which periodic AGN activity is assumed to cause bulk oscillations, rather than removal, of gas. See also discussion in Potzen & Governato 2012.

- Benson A. J., Bower R. G., Frenk C. S., Lacey C. G., Baugh C. M., Cole S., 2003, *ApJ*, 599, 38
- Benson A. J., Pearce F. R., Frenk C. S., Baugh C. M., Jenkins A., 2001, *MNRAS*, 320, 261
- Blumenthal G. R., Faber S. M., Flores R., Primack J. R., 1986, *ApJ*, 301, 27
- Brammer G. B., et al., 2011, *ApJ*, 739, 24
- Bryan G. L., Norman M. L., 1998, *ApJ*, 495, 80
- Buote D. A., Humphrey P. J., 2012, *ASSL*, 378, 235
- Cano-Diaz M., Maiolino R., Marconi A., Netzer H., Shemmer O., Cresci G., 2011, arXiv, arXiv:1112.3071
- Cattaneo A., et al., 2007, *MNRAS*, 377, 63
- Cattaneo, A., et al. 2006, *MNRAS*, 370, 1651
- Ciotti L., Ostriker J. P., Proga D., 2009, *ApJ*, 699, 89
- de Blok W. J. G., 2010, *AdAst*, 2010
- de Souza R. S., Rodrigues L. F. S., Ishida E. E. O., Opher R., 2011, *MNRAS*, 415, 2969
- Dubinski J., Carlberg R. G., 1991, *ApJ*, 378, 496
- Duffy A. R., Schaye J., Kay S. T., Dalla Vecchia C., Battye R. A., Booth C. M., 2010, *MNRAS*, 405, 2161
- Fabian A. C., 1999, *MNRAS*, 308, L39
- Fontanot F., De Lucia G., Monaco P., Somerville R. S., Santini P., 2009, *MNRAS*, 397, 1776
- Gnedin O. Y., Ceverino D., Gnedin N. Y., Klypin A. A., Kravtsov A. V., Levine R., Nagai D., Yepes G., 2011, arXiv, arXiv:1108.5736
- Gnedin O. Y., Kravtsov A. V., Klypin A. A., Nagai D., 2004, *ApJ*, 616, 16
- Gnedin O. Y., Zhao H., 2002, *MNRAS*, 333, 299
- Governato F., et al., 2010, *Natur*, 463, 203
- Granato G. L., De Zotti G., Silva L., Bressan A., Danese L., 2004, *ApJ*, 600, 580
- Granato G. L., Silva L., Monaco P., Panuzzo P., Salucci P., De Zotti G., Danese L., 2001, *MNRAS*, 324, 757
- Helly J. C., Cole S., Frenk C. S., Baugh C. M., Benson A., Lacey C., Pearce F. R., 2003, *MNRAS*, 338, 913
- Hernquist L., 1990, *ApJ*, 356, 359
- Inoue S., Saitoh T. R., 2011, *MNRAS*, 418, 2527
- Johansson, P.H., Naab, T., & Burkert, A. 2009, *ApJ*, 690, 802
- Kazantzidis S., Magorrian J., Moore B., 2004, *ApJ*, 601, 37
- Klypin A., Trujillo-Gomez S., Primack J., 2010, arXiv, arXiv:1002.3660
- Komatsu E., et al., 2009, *ApJS*, 180, 330
- Lapi A., Cavaliere A., 2011, *ApJ*, 743, 127
- Macciò A. V., Stinson G., Brook C. B., Wadsley J., Couchman H. M. P., Shen S., Gibson B. K., Quinn T., 2012, *ApJ*, 744, L9
- Martizzi D., Teyssier R., Moore B., Wentz T., 2011, arXiv, arXiv:1112.2752
- Mashchenko S., Wadsley J., Couchman H. M. P., 2008, *Sci*, 319, 174
- Mashchenko S., Couchman H. M. P., Wadsley J., 2006, *Natur*, 442, 539
- Memola E., Salucci P., Babić A., 2011, *A&A*, 534, A50
- Monaco, P., Fontanot, F., & Taffoni, G. 2007, *MNRAS*, 375, 1189
- Moster, B.P., et al. 2010, 710, 903
- Navarro, J.F., Frenk, C.S., & White, S.D.M. 1997, *ApJ*, 490, 493
- Navarro J. F., Eke V. R., Frenk C. S., 1996, *MNRAS*, 283, L72
- Newman A. B., Ellis R. S., Bundy K., Treu T., 2011, arXiv, arXiv:1110.1637
- Ogiya G., Mori M., 2011, *ApJ*, 736, L2
- Pasetto S., Grebel E. K., Berczik P., Spurzem R., Dehnen W., 2010, *A&A*, 514, A47
- Peirani S., Kay S., Silk J., 2008, *A&A*, 479, 123
- Pipino A., Silk J., Matteucci F., 2009, *MNRAS*, 392, 475
- Pontzen A., Governato F., 2012, *MNRAS*, 2641
- Pooley D., Rappaport S., Blackburne J. A., Schechter P. L., Wambsganss J., 2012, *ApJ*, 744, 111
- Ragone-Figueroa C., Granato G. L., 2011, *MNRAS*, 414, 3690
- Read J. I., Gilmore G., 2005, *MNRAS*, 356, 107
- Richtler T., Salinas R., Misgeld I., Hilker M., Hau G. K. T., Romanowsky A. J., Schuberth Y., Spolaor M., 2011, *A&A*, 531, A119
- Salucci P., Frigerio Martins C., 2009, *EAS*, 36, 133
- Sijacki D., Springel V., Di Matteo T., Hernquist L., 2007, *MNRAS*, 380, 877
- Silk J., Rees M. J., 1998, *A&A*, 331, L1
- Somerville R. S., Hopkins P. F., Cox T. J., Robertson B. E., Hernquist L., 2008, *MNRAS*, 391, 481
- Sonnenfeld A., Treu T., Gavazzi R., Marshall P. J., Auger M. W., Suyu S. H., Koopmans L. V. E., Bolton A. S., 2011, arXiv, arXiv:1111.4215
- Springel V., 2005, *MNRAS*, 364, 1105
- Tonini C., Lapi A., Salucci P., 2006, *ApJ*, 649, 591
- Tortora C., La Barbera F., Napolitano N. R., de Carvalho R. R., Romanowsky A. J., 2012, arXiv, arXiv:1201.2945
- Treu T., Auger M. W., Koopmans L. V. E., Gavazzi R., Marshall P. J., Bolton A. S., 2010, *ApJ*, 709, 1195
- Viola M., Monaco P., Borgani S., Murante G., Tornatore L., 2008, *MNRAS*, 383, 777
- Zhao, D.H., Mo, H.J., Jing, Y.P., & Börner, G. 2003, *MNRAS*, 339, 12
- Zitrin A., et al., 2011, *ApJ*, 742, 117